Crack Propagation Behavior in S15C and S35C after Overload

琉球大学工学部紀要　第68号，2007年

Bull.Fcculty of Engineering,Univ. of the Ryukyus No.68,2007

Crack Propagation Behavior in S15C and S35C after Overload

Anindito PURNOWIDODO[1], Takeo HISAI[2], Shingo FUKUZATO[3] and Chobin MAKABE[4]

[1]Mechanical Engineering Department, Brawijaya University, Jl. MT. Halang, East Java, 65145, Indonesia

[2]Japan Transocean Air Co., 3-24, Yamashita, Naha, Okinawa, 900-0027, Japan

[3]Okinawa Electric Power Co., 5-2 Makiminato, Urasoe, Okinawa, 901-2602 , Japan

[4]Mechanical Systems Engineering Department, University of the Ryukyus, 1 Nishihara, Okinawa, 903-0213, Japan

Abstract

Crack propagation is retarded after applying a tensile overload, and accelerated after applying a compressive overload in fatigue tests under constant base stress amplitude. However, at a negative value of the baseline stress ratio, the fatigue crack propagation rate can accelerate after applying a tensile overload. To evaluate such crack propagation behavior, the effective stress intensity factor range has been employed. The transition of residual fatigue life after applying these loads was observed and this behavior was dependent on the loading conditions. When the applied overload level was lower than a critical level, retardation of crack propagation was observed. However, when the applied overload level was higher than a critical level, the crack growth rate got higher. These phenomena are related to not only residual stress, but also crack opening behavior.

Key words: Fatigue crack, Crack propagation rate, Overload, Deceleration, Acceleration, Effective stress intensity factor range

1. Introduction

One of the causes of variation in crack propagation rate during service load application to engineering materials is plastic-induced crack closure that was originally introduced by Elber [(1)]. Although applying overloads, the crack propagation law can be evaluated by the effective stress intensity factor range, which is calculated using the crack opening stress [(2-8)]. A yield strength level is the most important material property affecting the extent of overload-related retardation when a plasticity-induced closure occurs. At the higher of the yield stress, the smaller the size of the plastic zone is obtained. As a result, the less extent of retardation is observed. However, in the case of negative stress ratio, the effect of plastic size is not yet known exactly. In the present study, the effect of overload to the behavior of crack propagation was investigated using carbon steels, S15C and S35C, and the effect of yield strength or plastic zone size on the crack propagation after an overload was investigated. Also, the crack propagation date da/dN as function of $(\Delta K_{eff}-\Delta K_{effth})^2$ proposed by McEvilly et al [(2, 3)] was examined.

2. Materials and Testing procedure

The materials used in the present study were two carbon steels, those are, 0.36 % and 0.15 % carbon steel. The chemical compositions and mechanical properties of the materials are shown in Tables 1 and 2, respectively. The shape of the specimen used is shown in Figure 1. The notch of 2.5 mm in length with 0.1 mm root radius was cut in the center of the flat section of the specimen by an electrical discharge machine. After being polished by using an emery paper and a metal polisher, the 1 mm of initial crack was introduced from the notch roots by a push-pull hydraulic fatigue test machine. The crack length, $2a$, is defined including the notch length, thus, the initial crack length was about 6 mm. This specimen was regarded as center-cracked plate. The fatigue crack propagation test was carried out using a hydraulic testing machine with cyclic frequency 10 Hz in laboratory room condition. The crack length, a, function of the number of cycles, N, was determined using the aid traveling microscope with accuracy 10 μm at the surface of the specimen. When the semi-crack length was reached 3 mm, a single overload was applied manually and then the constant stress amplitude was resumed.

Table 1 Chemical composition (% wt)

Material	C	Si	Mn	P	S	Ni	Fe
S35C	0.36	0.17	0.70	0.019	0.016	0.04	Bal.
S15C	0.15	0.30	0.50	0.013	0.013	0.05	Bal.

受理:2006年12月27日
平成15年10月2日,破壊力学シンポジウム内で発表済み
＊工学部機械システム工学科
(Mechanical Systems Engineering Department)

Table 2 Mechanical Properties

Material	σ_S,MPa	σ_BMPa	σ_TMPa	ϕ, %
S35C	292	493	975	62
S15C	283	449	956	69

σ_S : Lower yield strength, σ_B : Tensile strength
σ_T : True fracture stress, ϕ: Reduction of area

Table 3 shows the testing conditions. Figure 2 shows schematic representation of the applied cyclic stress. The stress ratio R is defined as the ratio of the minimum cyclic stress S_{min} to the maximum cyclic stress S_{max}, S_a is the stress amplitude, and S_{ov} is the overload stress. The percentage of overload is defined as follow.

$$\%Overload=\frac{K_{maxov}-K_{maxb}}{K_{maxb}-K_{minb}}x100\% \qquad (1)$$

where, $K_{max\,ov}$ is the stress intensity factor at the overload point, and $K_{min\,b}$ and $K_{max\,b}$ are the stress intensity factor at the minimum and maximum constant cyclic loading, respectively. To detect the crack opening and closing points, the local strain was measured by strain gage pasted on specimen center axis.

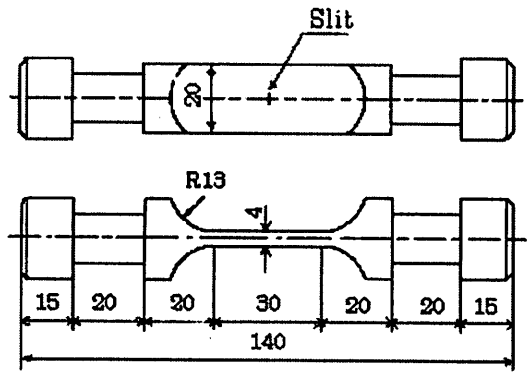

Fig. 1 Shape of Specimen

Table 3 Testing conditions where R was constant.

No	R	S_a MPa	S_{max} MPa	Tensile S_{OL} MPa	% Overload	Material
1	0	43	86	172	100	S35C
2	0	43	86	163	90	S15C
3	0	43	86	185	115	S15C
4	-1	67	67	180	85	S35C
5	-1	67	67	170	55	S15C
6	-1.5	85	67	184	77	S35C
7	-1.5	85	67	160	55	S15C
8	-1.5	85	67	178	66	S15C

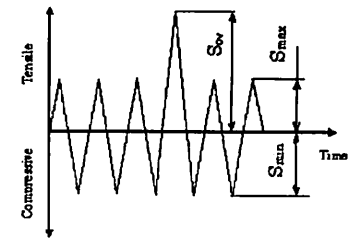

Fig. 2 Schematic representation of the applied cyclic stress

In addition, to know the effects of loading condition after the overload on crack propagation behavior, one of test was carried out under conditions that the stress ratio R after the overloading was changed from that before overload. This testing conditions is shown in Table 4. R_1 and R_2 are stress ratio before and after the overload as well as S_1 and S_2, respectively. The schematic representation of the loading cycles for the testing is illustrated in Fig. 3.

Table 4. Testing conditions where R was changed (S15C).

No	R_1	R_2	S_{a1} MPa	S_{max1} MPa	S_{a2} MPa	S_{max2} MPa	S_{OL} MPa	% Over load
9	0	-1.5	43	86	85	67	180	85
10	-1.5	0	85	67	43	86	180	85

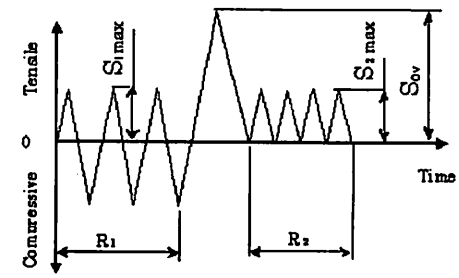

Fig. 3. Schematic representation of the loading cycles in Table 4.

3. Experimental results.

Figure 4 shows crack propagation curves for R=0, -1 and -1.5, respectively, the arrow shows the overload point. In the case of R=0, the usual retardation phenomenon occurs on both S35C, and S15C. The applied cyclic maximum stresses are same in all cases, since the S35C has higher yield strength, however, the effect of the overload to the extent of retardation in S35C is less than in S15C. In S15C, the retardation cycle was longer when the applied single overload was higher. Where specimen No.2, % overload = 905 %, and where specimen No.3, % overload = 115 %. This behavior is also related to the

plastic zone size created by static overload. In the case of R=-1, the retardation phenomenon associated with a tensile overload is less pronounced, however, the small succeeding retardation behavior is observed following the overload. In the case of R=-1.5, the usual retardation does not occur after the overload for some conditions but the crack growth actually accelerates on S35C specimens. At the higher overload level of S15C (specimen No.8, % overload = 66%), the acceleration of the crack growth was also observed. However, the retardation phenomenon occurs at lower overload level (specimen No.7, % overload = 55 %).

Figure 5 shows the crack propagation rate, *da/dN*, as function of the semi crack length, *a*, for stress ratio of 0, -1 and -1.5. Where stress ratio R =0, a very short period of acceleration just after application of the overload is observed. After reaching maximum value of the crack growth rate, the rates decelerates to the minimum value. These tendencies were the same in both cases of S15C and S35C. However, the maximum and minimum level of *da/dN* is different in both cases relating to the yield stress level. In the case of R=-1, from the crack propagation curves, the effect of the overload to the retardation is less pronounced. This is appeared on *da/dN-a* relation. Thus, the gradient of *da/dN-a* after maximum *da/dN* is smaller than that of the curve of R=0. In the case of stress ratio R=—1.5, after reaching maximum of *da/dN*, the crack growth rate gradually decreases to its base rate level. This

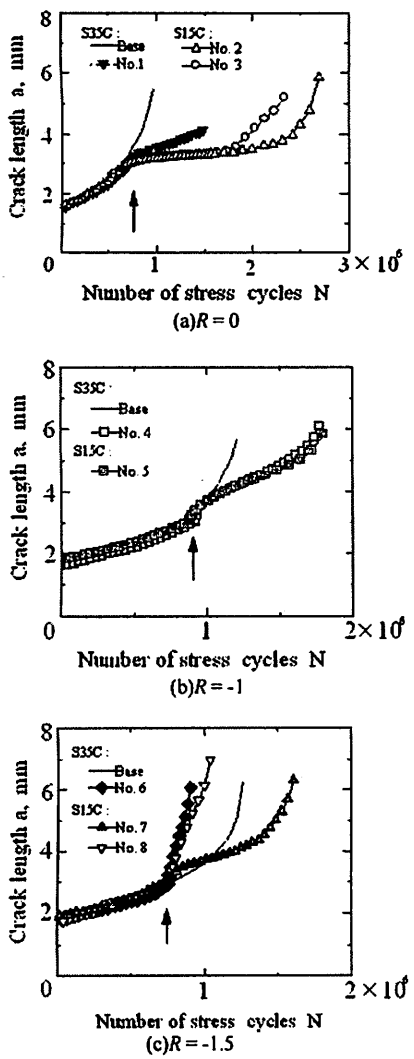

Fig. 4 Semi-crack length as a function of the number of constant amplitude cycles applied

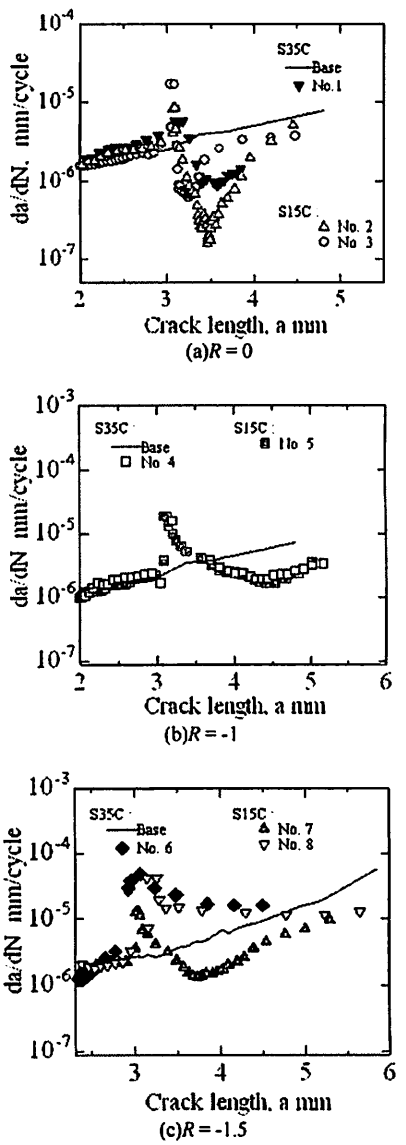

Fig. 5 Crack propagation rate *da/dN* as a function of crack length *a*.

acceleration phenomenon takes place on the both S35C and high % overload level of S15C.

Generally, crack propagation rate is evaluated by utilizing the stress intensity factor in the case of small scale yielding conditions. Figure 6 shows relationship between the crack propagation rate, *da/dN*, and maximum stress intensity factors, K_{max}, during cycled under stress ratio R= 0, -1, and –1.5 with the single tensile overload, respectively. The stress intensity factor was calculated by following equation.

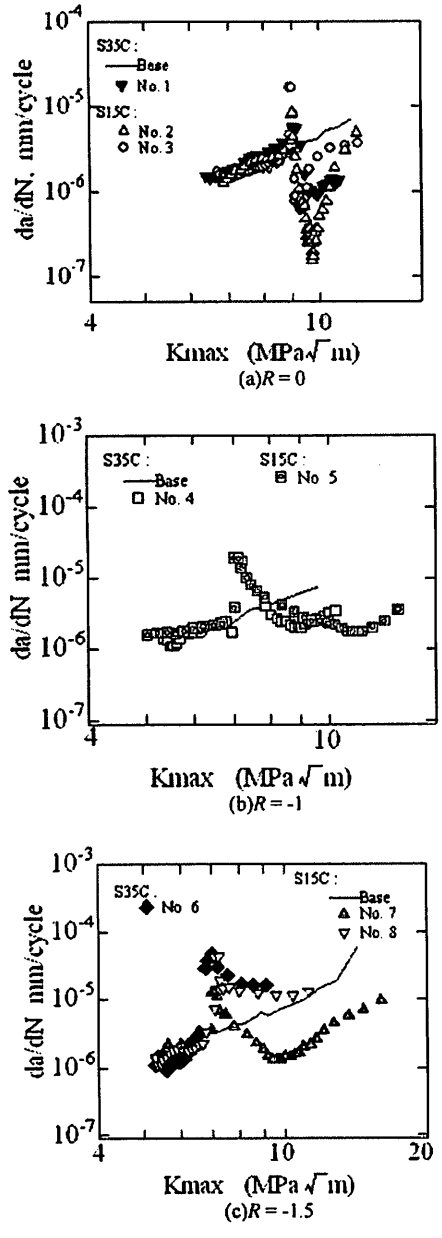

Fig. 6 Relation between *da/dN* and maximum stress intensity K_{max} for the single tensile overload

$$K = F(a/W)\sigma\sqrt{\pi a}$$

$$F(a/W) = \left\{1 - 0.025(2a/W)^2 + 0.064(2a/W)^4\right\}\sqrt{\sec(\pi(a/W))} \quad \cdots (2)$$

where, σ is the cyclic stress, a is the half crack length and W is the half specimen width. Crack propagation rate does not vary linearly as function of K_{max} in each stress ratio cases. Therefore, if a history load is taken into consideration, an evaluation to crack propagation rate using K_{max} had better to be not used.

Paris and Hermann [4] showed that the rate of fatigue crack propagation through the overload region is related to the effective stress intensity factor range. Therefore, the relation of crack propagation rate and maximum stress intensity factors are improved by using the effective stress intensity factor range, $\Delta K_{eff} = K_{max} - K_{op}$; K_{op} is the stress intensity factor at the crack opening level. To detect the crack opening point, subtracted-displacement method [9] was employed. Figure 7 shows an example of subtracted displacements vs. load for the specimen No 5 (R = -1, % overload = 55 %).

The loops in Fig. 7 were obtained when the crack tip was traversing prior to the overload (a=2.72 mm), within the overload zone (a=3.25 mm & a=3.32 mm), and when the crack tip was emerging from the overload zone (a=4.00 mm & a=4.20 mm). The crack opening level, S_{op}, is higher before the crack tip penetrated to the overload zone, and in the overload zone, the opening level of crack is reduced. Also, when the crack tip was with the overload plastic zone, two crack opening level were measured. The upper level S_{op2} is employed as the opening point at the surface in the present study. After the crack tip traversed overload zone, the crack opening level becomes higher than in the overload zone. This crack opening behavior relates to the plastic

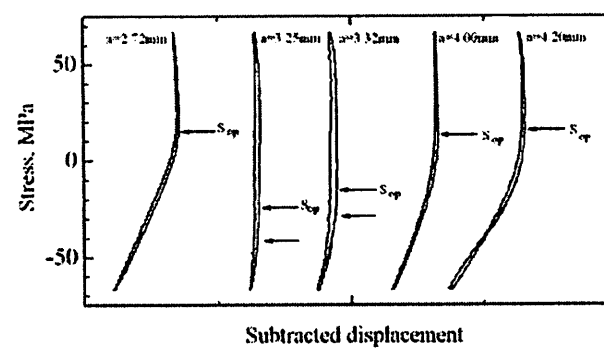

Fig. 7. Example of load vs. subtracted displacement plots (R=-1.0, Specimen No.5).

deformation caused by the overload in the vicinity of crack tip. The example variation of crack opening level all experimental curves are shown in Fig. 8.

Figure 9 shows unique relationships between crack propagation rate *da/dN* and ΔK_{eff}, which is independent of stress ratios and the overload values. It means that the crack propagation is controlled by the crack closure, even if the cyclic loading is applied by such conditions as the overload level is exceed over the small scale yielding condition, and as the crack propagation rate is decelerate or accelerate by the applying overload.

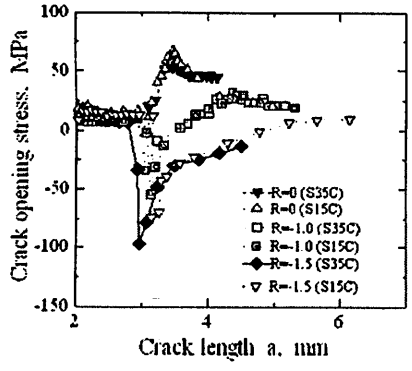

Fig. 8. Variation of the crack opening stress level following an overload at three baseline *R* levels.

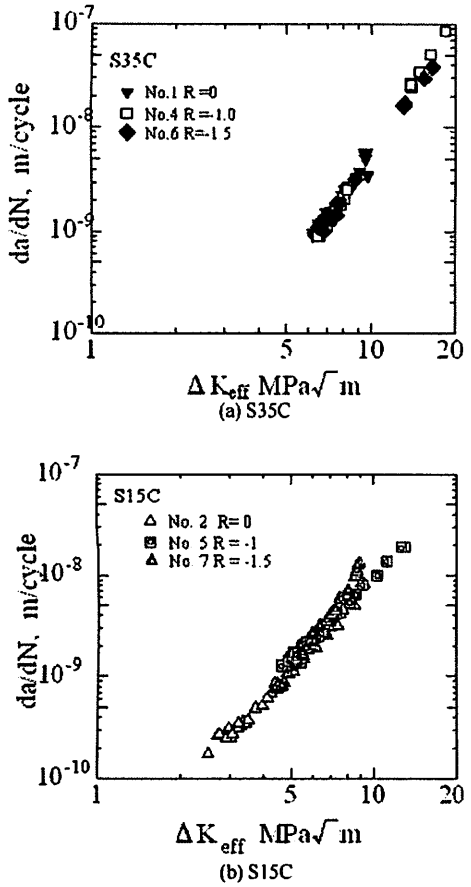

Fig. 9 Relation between *da/dN* and effective stress intensity factor ΔK_{eff} for the single tensile overload

4. Discussion

4.1 Crack tip condition after an overload

As reported by McEvily et al [2,3] that principal causes of the crack retardation following an overload at stress ratio greater than zero is the lateral contraction of material in the plane-stress that occurs on the overload zone surface. When the overload is applied, the material in the zone of front of crack tip will be deformed plastically because of the high stress concentration. The deformation process is not reversible upon unloading to minimum load from overload level, and as the result, the material element in the plastic zone has been permanently extended in the loading direction. This material extension gives rise to the development compressive residual-stress at the crack tip upon unloading to the minimum load of the cycle. As the fatigue crack tip penetrates through this zone, the residual stress is relaxed when the crack is fully opened. However, in order to relax the residual compressive stress, the element material must extend elastically, and this extension enhances crack closure level in crack wake of the crack tip during unloading. In addition, because of the higher-level crack closure

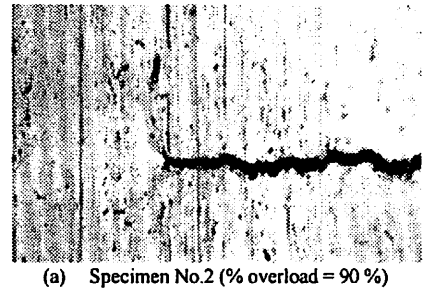

(a) Specimen No.2 (% overload = 90 %)

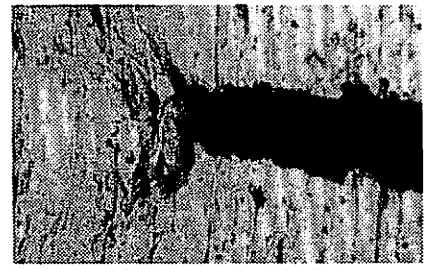

(b) Specimen No. 3 (% overload = 115 %)

Fig. 10 Crack tip conditions in S15C, *R*=0..

existing in the behind of crack tip as the crack grows through the overload zone, the crack opening level in the region is higher than elsewhere. Accordingly, the condition of the zone serves to retard the rate of crack propagation.

The overload plastic zone size, which is related to yield strength and applied overload stress level, affect the crack propagation life after overload. Thus, the crack tip deformation just after applying is investigated. Figure 10 shows the examples of deformation at R=0 in the case of the S15C specimens [No.2 (% overload = 90 %), No.3 (% overload = 115 %)]. The differences of fatigue life occurred and that was caused by crack tip condition at the point of the application of the overload. With lower overload level (specimen No.2), the relatively small crack tip opening displacement at the overload point is, and the fatigue life and the crack growth rate became longer and slower, respectively. When the crack tip displacement was larger (specimen No.3), the fatigue life and the crack growth rate became shorter and faster than No.2, respectively. Therefore, it is found that the crack-tip condition after the application of the overload influenced crack propagation behavior.

As previously mentioned that the retardation of fatigue crack growth did not occur following an overload at some cases of R= -1.5. Thus, after application of an overload, the crack rate accelerated immediately, and fatigue life became shorter than the case of base without the overload application. This behavior was associated with the conditions of the plastic zone ahead the crack tips. Upon unloading from overload level to zero load, the compressive residual stress developed in the plastic zone. However, repeating application of compression stress after overload brought the change of residual stress condition depending on the compression stress level. If the locally compressive load was high enough, the affected zone by overload would be yield again, and bulge would be started to develop. The magnitude of the bulge increased as the minimum load level increased [7]. The bulge indicated that there was material movement to outward, so it reduced crack closure level behind the crack tip. Upon returning to zero load, the overload zone was in state of tension residual stress rather than compression residual stress. Therefore, these factors lead to acceleration of the fatigue crack.

In the present study, not all loading conditions of negative stress ratio led to acceleration of the crack. The retardation of crack growth occurred on the S15C material with lower overload level. In the case of the No.7, the crack tip displacement at overload point was relatively small. Hence, the crack face behind the crack tip contacted each other during recycled with constant stress amplitude. This condition did not cause the severe stress concentration under the compression stress, so the bulging of material did not occurred. Also, when the crack penetrated through the overload zone, the compression residual stress relaxed, which enhanced the crack closure behind the crack tip. Figure 11 shows the crack tip conditions of the specimen No 7 (S15C, % overload = 55 %), at the point overload and after 4000 cycles from the overload application. It can be observed that at that stage closed by maximum compression stress, the crack surface behind the point at which the overload was applied. Conversely, in the specimen with that large crack tip deformation occurred (specimen No.8), the crack faces behind its crack tip following the overload was not contacting each other when the specimen was recycled in constant amplitude load as shown in Fig.12. Because of the condition behind the crack tip and the residual stress in the overload zone, the local compressive stress in the vicinity ahead of crack tip was in higher level

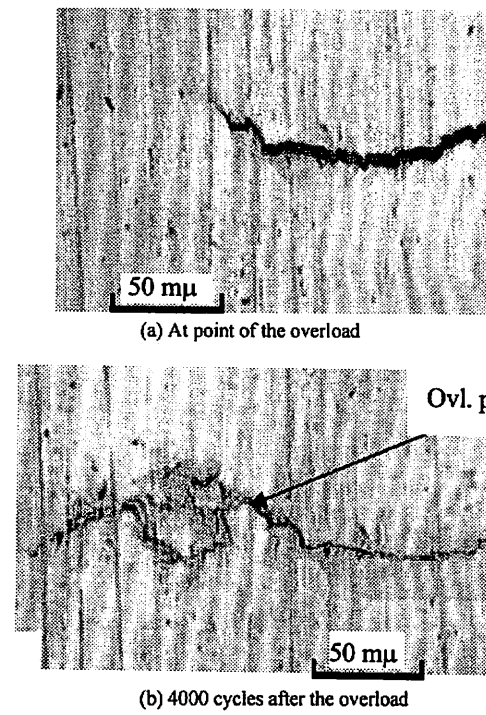

(a) At point of the overload

(b) 4000 cycles after the overload

Fig. 11. Crack tip conditions of specimen No 7 (S15C), R=-1.5.

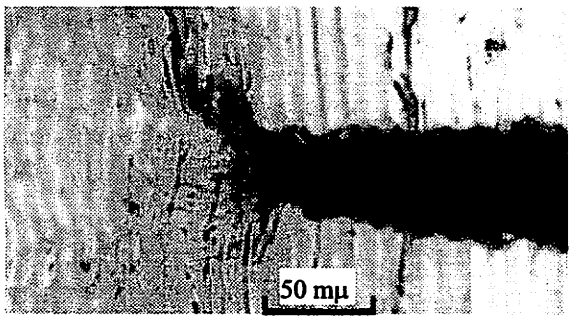

(a) At point of the overload

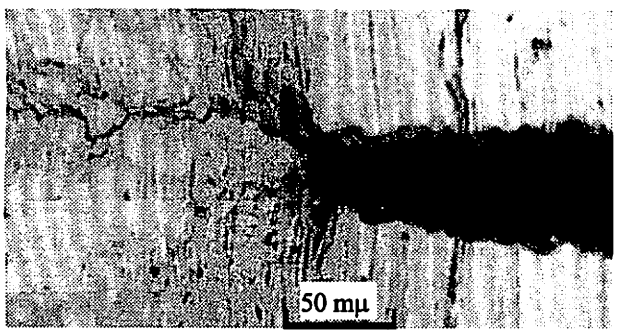

(b) 5000 cycles after the overload

Fig. 12. Crack tip conditions of specimen No. 8 (S15C), R =-1.5.

than elsewhere, when the specimen was loaded to the minimum load under stress ratio of –1.5 level. The higher compressive stress caused material bulging in the overload zone, and local material leading to serve crack closure was forced to outward direction. Afterward, upon unloaded from the minimum load level to zero load, tensile residual stress developed in the overload zone. Therefore, the conditions of crack tip influence also crack propagation behavior on subsequent cycles after an overload under stress ratio R= 1-5.

In the case of stress ratio R= -1, as mentioned before, the effect of the tensile overload was less pronounced. Although, the plastic zone created by the overload was in the same manner as on the stress ratio R= 0, the compression residual stress distributing changed to tensile residual stress just after the application of the overload. However, during the crack propagation, the distribution of the residual stress changed, and after some length of crack growth, the tensile residual stress changed to the compression again.

4.2 Effects of loading conditions on crack propagation after overloading

To confirm the effect of succeeding loading conditions on the crack propagation behavior after the application of overload, different stress ratios between before and after the application of overload were investigated (The testing condition and schematic representation of the applied cyclic stress are shown in the Table 4 and Figure 3, respectively).

The effect of the constant cyclic load condition can be observed in Figure 13. In the case of specimen No.9 (%overload = 85%, R_1= 0, R_2= -1.5), which was loaded in constant cyclic load under stress ratio R= 0 before overload, and continued with stress ratio R=-1.5 after application of the overload, the fatigue life become shorter. However, in the case of specimen No.10 (%overload= 85%, R_1= -1.5, R_2= 0) the delay phenomenon of crack growth was observed when it was loaded in the constant amplitude with R= 0 following the overload, although before the overload had been cycled in constant load with R= -1.5.

The deceleration or acceleration can be clearly observed in the rate of crack growth, da/dN, as a function of crack length, a, as shown in the Fig. 14 in which the constant cyclic load conditions after the overload have important role to determine whether the rate of crack. decelerate or accelerate. However, the crack propagation

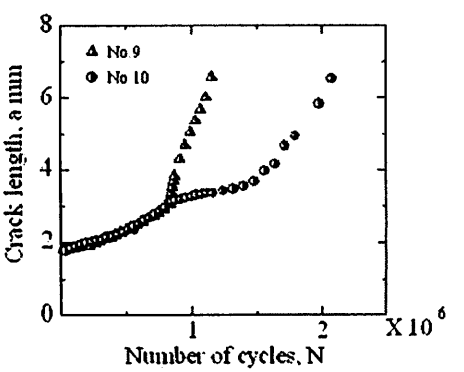

Fig. 13. Relationship between number of cycles and crack length

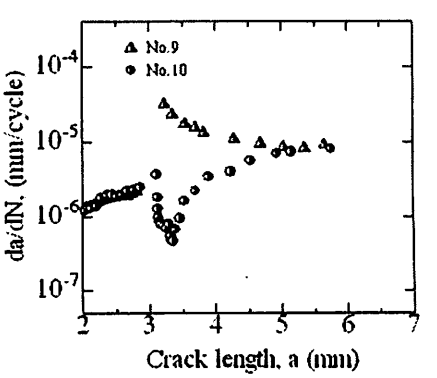

Fig. 14 Relationship between crack growth rate and crack length.

behavior post the overload is independent of the cyclic load condition prior the overload. In these cases, therefore, the distribution of the residual stress in the vicinity of the crack tip is depended on the stress amplitude condition following of the overload, also

In the acceleration case (specimen No 9), which was loaded with stress ratio R= 0 before the overloading, and then continued with the stress ratio R= -1.5 after the overload, the tensile residual stress developed in the front of the crack tip region in the subsequent cyclic after the overload. Consequently, the crack opening stress level in the region became low and after reaching the lowest value of crack opening stress, the crack opening returned gradually to the basic opening stress level when the crack emerged from the effected overload zone. In contrast, the crack opening stress increased in the effected overload zone in the case of specimen No 10, which was cyclic in constant stress amplitude with stress ratio R = -1.5 before the overload, and with stress ratio R = 0 after the overload. After the crack tip traversed the overload zone, the crack opening stress returned to the basic crack opening level. The variation of the crack opening stress is shown in the Fig.15. Besides the crack tip condition, the crack propagation behavior following the overload is influenced also by stress cycles condition since it will change the residual stress state that develops in the front of crack tips.

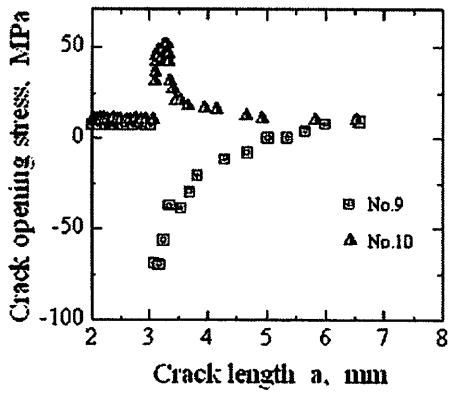

Fig. 15 Variation of crack opening stress.

4.3 Evaluation of crack propagation rate by effective stress intensity factor range.

The same as reported in the previous chapter that the retardation or acceleration of the crack propagation after the overload is dependent on the stress ratio R, and the overload level. This is similar to the crack tips conditions effects residual stress distribution in succeeding cycle.

The rate of crack propagation in the overload zone is related to the value of ΔK_{eff}, and the following constitutive equation for the rate of fatigue crack propagation has been proposed by McEvily et al.[2,3].

$$\frac{da}{dN} = A(\Delta K_{eff} - \Delta K_{effth})^2 \qquad (3)$$

where A is a material constant, and ΔK_{effth} is the value of ΔK_{eff}, at the threshold level. In this study, da/dN of the threshold value was defined as 10^{-11} m/cycle, and ΔK_{effth}, was found to be 3 MPa $\sqrt{m}$ for S35C, and 2.5 MPa$\sqrt{m}$ for S15C. According to Eq. (3), the log of the rate of fatigue crack growth should vary linearly as a function of the quantity in parentheses in Eq. (3) and the slope of this linear relation should be 2.0, independent of R value, mechanical property and loading history. Figure 16 shows the results of the present investigation in the overload regions plotted in this manner, and it is seen that there is reasonable agreement between Eq. (3) and these results.

When a tensile overload is applied at a baseline loading level of R= -1.5, the residual compressive stress created on unloading from the overload level is changed to a residual tensile stress by the R=-1.5 cycling, and the crack growth rate is accelerated rather than being retarded, and this behavior occurred on both S15C and S35C. However, the retardation or acceleration of the crack not only depend on stress ratio and overload level but also crack tip condition after the overload, which influence residual stress state in front of the crack tip. Unless this effect taking into account, an non-conservative estimation of the fatigue life for components subjected to such a loading history will be made.

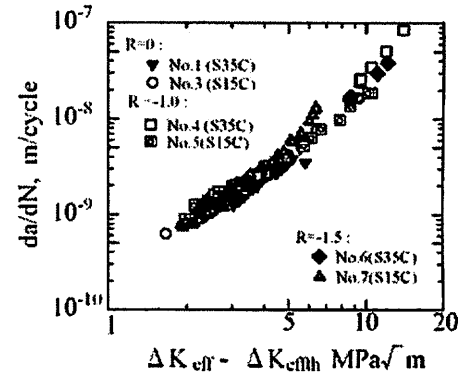

Fig. 16. Rate of fatigue crack growth following an overload as a function of the parameter $\Delta K_{eff} - \Delta K_{effth}$.

4.4 Delay and acceleration Cycles

The number of delay cycles, N_D, and the delay length, a_D associated with the overload application during a constant stress amplitude test are defined as in the Fig. 17. Figure 18 shows typical variation in the rate of fatigue crack growth as the crack tip penetrates the overload zone. When the crack propagation accelerates after overload, fatigue life become shorter than base testing without overloading. To define the shortening cycles by *a-N* curve is difficult. We called this cycle as acceleration cycle, N_{AC}, and determined this using *da/dN-N* curve. Figure 19 shows the example of the *da/dN* and *N* relation. The acceleration cycles N_{AC}, is defined as the subtraction the number of stress cycles of overloading test from that of the baseline at which the crack propagation rate da/dN reached minimum value after applying overload. Figure 20 shows schematic representation of the relation between da/dN, and definition of N_{AC}.

Table 5 shows the result of predicted number of delay cycles and acceleration cycles according to the definitions as shown in Figure 17 and 20, respectively. The negative sign for number of cycles, *N*, denotes number of cycles acceleration. A prediction of number of delay cycles, N_D, following an overload has been proposed by Bao and McEvily [3] as Eq. (4).

$$N_D = \frac{OLPZ}{A\left(K_{mak}-K_{op2max}-\Delta K_{effth}\right)\left(K_{mak}-K_{opb}-\Delta K_{effth}\right)} \frac{OLPZ}{A\left(K_{mak}-K_{opb}-\Delta K_{effth}\right)^2} \quad (4)$$

where A is the material constant, ΔK_{effth} is the effective stress intensity factor range ΔK_{eff} at the threshold level, which is taken to correspond to a growth rate of 10^{-11} m/cycle, K_{maxb} is maximum stress intensity factor in baseline condition, K_{opb} is the opening level of K_{maxb}, and in the overload zone, the K opening level is K_{op2max} corresponding to the minimum crack growth rate. The first on the right hand side of Eq.4 represents the total

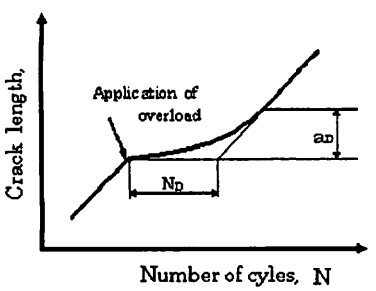

Fig. 17. Definition of the number of delay cycle

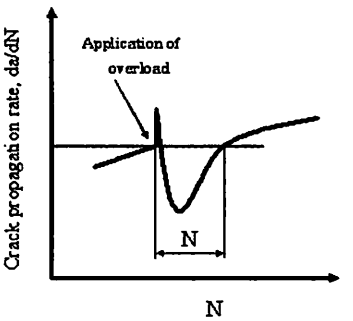

Fig. 18. Characteristic feature of crack growth rate post-overload

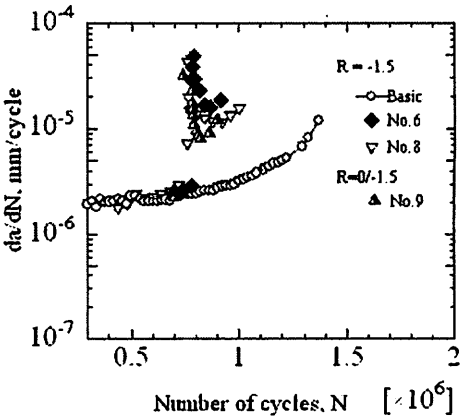

Fig. 19. Relationship between crack propagation rate *da/dN* and number of cycles *N*

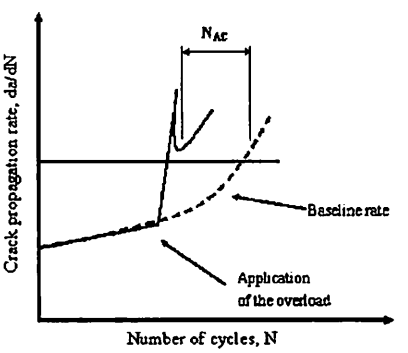

Fig. 20. Definition of the number of acceleration cycles

Table 5—Number of delay and acceleration cycles

Specimen Number	*R*	Number of delay or acceleration cycles	Material
1	0	740000	S35C
2	0	1600000	S15C
3	0	1090000	S15C
4	-1	770000	S35C
5	-1	840000	S15C
6	-1.5	-690000	S35C
7	-1.5	640000	S15C
8	-1.5	-500000	S15C
9	0/-1.5	-549000	S15C
10	-1.5/0	695000	S15C

number of cycles to traverse the overload plastic zone (*OLPZS*), and the second term is the number of cycles to traverse in the same distance in the absence of an overload.

The distance to the end of the overload effect is also material dependent. The following relation has been used to approximate this distance:

$$OLPZS = \frac{1}{\pi}\left(\frac{K_{ov}}{\sigma_Y}\right)^2 \qquad (5)$$

where, K_{ov}, is the stress intensity factor at the overload level, and σ_y is the yield strength.

In the present paper, the above equation is modified to take into account the baseline closure level, K_{opb}, as follows;

$$OLPZS = \frac{1}{\pi}\left(\frac{K_{ov} - K_{opb}}{\sigma_Y}\right)^2 \qquad (6)$$

In this study the prediction of number delay cycle, N_D, proposed by Bao and Mc.Evily [3] was examined. In the acceleration cases of crack growth rate following an overload, the K_{op2max} should correspond to the maximum rate in the overload zone. Figure 21 shows the rate of fatigue crack growth rate under constant load amplitude conditions as function of ΔK for R ratios of -1 and -1.5, also in the figure a calculated curve is shown, which is base upon Eq. (3). The constants used in the calculation are given in the Table 6, and the stress intensity factors for a center cracked plate is given as Eq.(2).

To predict the delay cycles, N_D, or acceleration cycles N_{AC} , the Eq. (4) was employed and the K values in the Table 7 were used in this calculation. Table 8 presents the results of the calculations and the experiment results for N_D and N_{AC}. It is considered that the calculated values of N_D and N_{AC} are in reasonable agreement with the experimental result.

Figure 22 shows the predicted number of delay cycles, N_D, as function ΔK_b of the baseline cycles, which was calculated base upon Eq.(4), and it is possible if $K_{op2,\,max}$ were known as a function of ΔK. In this present study, the following expression proposed by McEvilly et al [2,3] is used to determine $K_{op2,\,max}$ without considering the experimentally determined values.

$$K_{op2,\max} = 0.8\Delta K \qquad (7)$$

As shown in the Fig. 22, in the delay cases, the calculation results agrees quiet well with the experimental results for the number of different ΔK levels. However,

Table 6 Material Constants

Material	σ_y,MPa	A(MPa)^2	ΔK_{effth} MPa $\sqrt{m}$
S35C	292	3×10^{10}	3.0
S15C	283	3×10^{10}	2.5

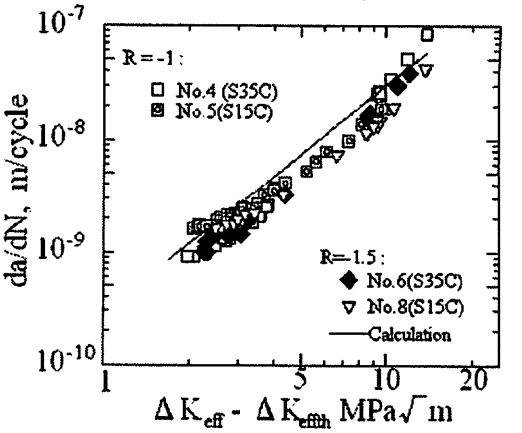

Fig. 21. Fatigue crack growth rate as function ΔK

Table 7. Stress Intensity factors* and OLPZS

No.	R	K_{max}	K_{opb}	ΔK_{effb}	K_{op2max}	K_{ov}	OLPZS	Material
1	0.0	9.44	1.90	7.54	5.30	21.75	0.00161	S35C
2	0.0	8.60	1.30	7.30	5.40	20.61	0.00159	S15C
3	0.0	8.69	1.30	7.39	5.10	23.40	0.00207	S15C
4	-1.0	6.79	1.20	5.59	2.30	22.76	0.00177	S35C
5	-1.0	6.70	0.80	5.90	2.80	21.50	0.00174	S15C
6	-1.5	6.80	1.07	5.73	-5.20	23.27	0.00185	S35C
7	-1.5	6.90	0.82	6.08	2.83	20.23	0.00153	S15C
8	-1.5	6.70	1.10	5.60	-5.50	22.51	0.00191	S15C
9	0 to -1.5	6.70	0.97	5.73	-6.20	22.76	0.00196	S15C
10	-1.5 to 0	8.60	1.70	6.90	4.20	22.76	0.00196	S15C

*Unit for K are MPa $\sqrt{m}$

Table 8 Calculated and Experimental Values of N_D and N_{AC}

Specimen Number	R	N_d or N_{ac} Exp (x 10^5)	N_d or N_{ac} Cal (x 10^5)	Ratio Calc./Exp.	Material
1	0	7.40	9.29	1.25	S35C
2	0	16.00	1.62	1.01	S15C
3	0	10.90	1.21	1.11	S15C
4	-1	7.70	7.77	1.01	S35C
5	-1	8.40	8.59	1.02	S15C
6	-1.5	-6.90	-6.91	1.00	S35C
7	-1.5	6.40	6.13	0.96	S15C
8	-1.5	-5.00	-5.41	1.08	S15C
9	0/-1.5	-5.49	-5.17	0.94	S15C
10	-1.5/0	6.95	5.32	0.76	S15C

Avg. = 1.02

where the crack growth was accelerated, the present prediction cannot be applied. It is caused by the determination method of the value $K_{op2,max}$ where $K_{op2,max}$ is negative. The method of this will be improved in the future.

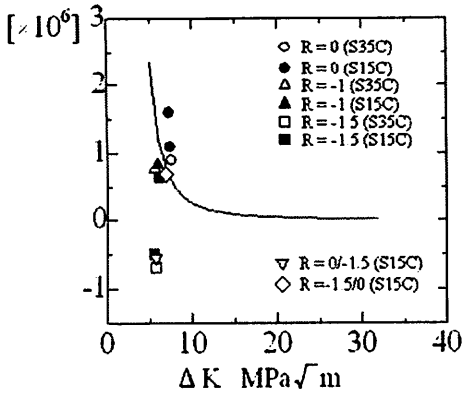

Fig. 22. Predicted number of delay cycles, N_D , and acceleration cycles, N_{AC}, as function of the baseline ΔK_b level.

5. Conclusion

Main results obtained in the present study are as follows:

(1) Crack propagation behavior after an application of the overload depends on the stress ratio R, overload level, crack tip condition and mechanical properties of the material.

(2) Where R value was zero, the crack closure induced by an overload retards the rate of fatigue crack growth. The retardation associated with the overload was more profound on the S15C than S35C because the yield strength of the S15C is lower than S35C. Also, where R value was -1, the retardation of the crack growth, which occurred on both S15C and S35C was observed. But, the retardation period at R=-1 was shorter than that at R=0.

(3) Where R value was -1.5, the crack closure induced by the overload can be eliminated and the rate of fatigue crack growth can be accelerated rather than being retarded. However, the acceleration or retardation that occurred is related to the crack tip condition after the overload

(4) The rate of fatigue crack growth as function of ΔK_{eff} - ΔK_{effth} is independent of the R value, the overload level and the mechanical properties.

(5) The crack propagation behavior after the overload is strongly influenced by the constant cyclic stress condition following the overload.

(6) The calculated number of delay cycles following an overload level has good agreement with experimental values.

References

[1] Elber, W., "The Significance of Fatigue Crack Closure," *Damage Tolerance in Aircraft Structures, ASTM STP 486*, American Society for Testing and Materials, Philadelphia, 1971, pp. 230-242.

[2] McEvily, A. J. and Yang, Z., "The Nature of the Two Opening Levels Following an Overload in Fatigue Crack Growth," *Metallurgical Transactions*, Vol. 21A, 1990, pp. 2717-2727.

[3] Bao, H. and McEvily, A. J., "The Effect of Overload on the Rate of Crack Propagation under Plane Stress Conditions," *Metallurgical and Materials Transaction*, Vol. 26A, 1995, pp. 1725-1733

[4] Paris, P. C. and Henman, L., "Twenty Years of Reflection on Questions Involving Fatigue Crack Growth, Part II: Some Observation on Fatigue and Fatigue Thresholds," *Proc. 1st Int. Conf. on Fatigue Thresholds*, Edited by Backlund, J., Blom, A. F. and Beevers, C. J., EMAS, Ltd., Warley, United Kingdom, Vol. 1, pp. 11-32 (1982)..

[5] Ward-Close, C. M., Blom, A. F., and Ritchie, R. O., "Mechanisms Associated with Transient Fatigue Crack Growth under Variable-Amplitude Loading: An Experimental and Numerical Study, " *Engineering Fracture Mechanics*, Vol. 32, 1989, pp. 613-638.

[6] Topper, T. H. and Lam, T. S., "Derivation of Crack Closure and Effective Fatigue Crack Growth Data from Smooth Specimen Fatigue Test," *Report of Fatigue Branch of the Society of Materials Science, Japan*, Vol. 266, 2003, pp. 1-12.

[7] Makabe, C., McEvily, A. J., Purnowidodo, A., and Yamauchi, A., "Effects of Negative Stress Ratios on Crack Propagation Behavior after an Overload," *Int. J. Modern Physics. B*, Vol. 17, 2003, pp. 1580-1586.

[8] Makabe, C., Purnowidodo, A., and McEvily, A. J., "Effects of Surface Deformation and Crack Closure on Fatigue Crack Propagation after Overloading and Underloading," *Int. J. Fatigue*, Vol, 26, 2004, pp. 1341-1348.

[9] Kikukawa, M., Jono, M., Tanaka, K., and Takatani, M., "Measurement of Fatigue Crack Propagation and Crack Closure at Low Stress Intensity Level by Unloading Elastic Compliance Method," *J. Society of Materials Science, Japan*, Vol.25, 1976, pp. 899-903.